Second Virial Coefficient and Gyration-Radius Expansion Factor of Oligo- and Poly(α-methylstyrene)s near the Θ Temperature

Tomoaki Kawaguchi, Masashi Osa, Takenao Yoshizaki, and Hiromi Yamakawa*

Department of Polymer Chemistry, Kyoto University, Katsura, Kyoto 615-8510, Japan

Received November 27, 2003

ABSTRACT: The second virial coefficient A_2 was determined for atactic oligo- and poly(α-methylstyrene)s (a-PαMS) in cyclohexane below, at, and above Θ (30.5 °C) in the range of weight-average molecular weight M_w from 5.30×10^2 to 3.22×10^6. The gyration-radius expansion factor α_S was also determined for the samples with $M_w \geq 4.07 \times 10^5$. It is found that A_2 increases rapidly with decreasing M_w for small M_w because of effects of chain ends. By the use of the theory recently developed on the basis of the helical wormlike chain model with consideration of effects of three-segment interactions in addition to those of chain ends, the effective excess binary-cluster integrals associated with the chain end beads and also the effective binary-cluster integral β between intermediate identical beads are determined as functions of the absolute temperature T. With values of β so determined, the conventional and scaled excluded-volume parameters z and $\tilde{z}$ near the Θ temperature are calculated. The behavior of the part $A_{2,\beta}^{(HW)}$ of A_2 without the effects of chain ends and three-segment interactions as a function of z and of α_S as a function of $\tilde{z}$ is examined for the present results for a-PαMS along with previous ones for atactic polystyrene. It is then found that the conclusions previously derived without consideration of the effects of three-segment interactions are still valid; i.e., (1) β is not proportional to $\tau = 1 - \Theta/T$ but is quadratic in τ below Θ in contrast to the result above Θ that $\beta \propto \tau$, (2) the result for the part $A_{2,\beta}^{(HW)}$ below Θ is consistent with the two-parameter theory prediction, and (3) the quasi-two-parameter theory is valid for α_S below Θ as well as above Θ.

Introduction

Recently, we have made experimental studies[1−3] of the second virial coefficient A_2 and gyration-radius expansion factor α_S for some typical flexible polymers and their oligomers near the Θ temperature within the framework of polymer solution theory on the basis of the helical wormlike (HW) chain model.[4] The findings of these studies may be summarized as follows: (1) The binary-cluster integral β_2 (between intermediate beads) determined from A_2 (for oligomers) with the correction for effects of chain ends is not proportional to $1 - \Theta/T \equiv \tau$ with T the absolute temperature but is quadratic in τ below Θ in contrast to the result above Θ that $\beta_2 \propto \tau$. (2) The result for the part $A_2^{(HW)}$ of A_2 without the effects of chain ends below Θ is consistent with the two-parameter (TP) theory prediction;[5] that is, the quantity $A_2^{(HW)}M^{1/2}$ with M the molecular weight (for a given polymer) is a function only of the conventional excluded-volume parameter z. (3) The quasi-two-parameter (QTP) theory[4] is valid for α_S below Θ as well as above Θ; that is, α_S is a function only of the intramolecular scaled excluded-volume parameter $\tilde{z}$.

In the above theory, excluded-volume interactions are considered in the binary cluster approximation.[5] As pointed out by Cherayil et al.[6] and by Nakamura et al.,[7] however, there are possible effects of three-segment interactions (ternary-cluster integral β_3) on A_2 near the Θ temperature where $\beta_2 \simeq 0$. If this contribution of β_3 is not negligibly small, we must make some modifications of the analysis made so far. Very recently, the HW theory of A_2 at the Θ temperature with the effects of three-segment interactions has been developed[8] by an extension of the random-flight chain theory,[9] where the effective binary-cluster integral β defined by $\beta = \beta_2 +$ constant. β_3 is used in place of β_2. It has then been shown that the new theory may give a rather satisfactory explanation of Monte Carlo data[8] and also very recent experimental data for A_2 for atactic oligo- and poly(α-methylstyrene)s (a-PαMS) in cyclohexane at 30.5 °C (Θ)[10] along with previous ones for atactic polystyrene (a-PS)[1,11] and atactic poly(methyl methacrylate)[2,12] at the respective Θ temperatures. In the present work we make an experimental study of A_2 and α_S of a-PαMS in cyclohexane near the Θ temperature on the basis of the new HW theory with consideration of the effects of three-segment interactions and examine whether the above-mentioned three findings (near Θ) are still valid. A reanalysis of the previous data for a-PS is also made along the new line.

We here note that Li et al.[13] have made a study of A_2 and the mean-square radius of gyration $\langle S^2 \rangle$ of PαMS in cyclohexane at and below the Θ temperature in the range of the weight-average molecular weight M_w from 6×10^4 to 10^6. However, it is not appropriate to use their values of A_2 and $\langle S^2 \rangle$ for the present purpose. The reasons for this are the following. First, our analysis requires data for the oligomers with very small M. Second, as previously[14] mentioned, their value 36.2 °C of Θ determined[15] so that the Houwink−Mark−Sakurada exponent becomes 0.5 is appreciably higher than our value 30.5 °C. Third, their values of $\langle S^2 \rangle / M_w$ for $M_w \gtrsim 10^6$ are 13% larger than ours.

Experimental Section

Materials. All the a-PαMS samples used in this work are the same as those used in the previous studies[10,16] of A_2 and the mean-square optical anisotropy, i.e., fractions separated by preparative gel permeation chromatography (GPC) or fractional precipitation from the original samples prepared by living anionic polymerization.[14,17] We note that the sample AMS40 is a fraction from the commercial sample 20538-2 from Polymer Laboratories Ltd. We also note that all the samples have a fixed stereochemical composition (the fraction

10.1021/ma035781d CCC: $27.50
Published on Web 02/24/2004

Table 1. Values of M_w and M_w/M_n for Atactic Oligo- and Poly(α-methylstyrene)s

sample	M_w	M_w/M_n
OAMS4	5.30×10^2	<1.01
OAMS5	6.48×10^2	<1.01
OAMS8	1.04×10^3	1.01
OAMS13	1.60×10^3	1.02
OAMS33	3.95×10^3	1.04
OAMS67	7.97×10^3	1.04
AMS2	2.48×10^4	1.02
AMS5	5.22×10^4	1.02
AMS15	1.46×10^5	1.02
AMS40	4.07×10^5	1.02
AMS200	2.06×10^6	1.05
AMS320	3.22×10^6	1.05

of racemic diads $f_r = 0.72$) independent of M_w, possessing a *sec*-butyl group at the initiating chain end and a hydrogen atom at the other end.

The values of M_w determined by analytical GPC or from light-scattering (LS) measurements (in cyclohexane at 30.5 °C) and the ratio of M_w to the number-average molecular weight M_n determined by analytical GPC are given in Table 1. As seen from the values of M_w/M_n, all the samples are very narrow in molecular weight distribution.

The solvent cyclohexane used for LS measurements was purified according to a standard procedure.

Light Scattering. LS measurements were carried out to determine A_2 for all the a-PαMS samples and $\langle S^2 \rangle$ for the three of them with the largest M_w in cyclohexane at various temperatures ranging from 15.0 to 45.0 °C. A Fica 50 light-scattering photometer was used for all the measurements with vertically polarized incident light of wavelength 436 nm. For a calibration of the apparatus, the intensity of light scattered from pure benzene was measured at 25.0 °C at a scattering angle of 90°, where the Rayleigh ratio $R_{Uu}(90°)$ of pure benzene was taken as 46.5×10^{-6} cm^{-1}.[18] The depolarization ratio ρ_u of pure benzene at 25.0 °C was determined to be 0.41 ± 0.01 by the method of Rubingh and Yu.[19]

The conventional method was used for solutions of the samples with $M_w > 10^3$, while the procedure previously[20] presented was applied to those of the oligomer samples with $M_w < 10^3$ as before[1−3,11,12] since then the concentration dependence of the density scattering R_d and of the optical constant K cannot be ignored in the determination of A_2 (and also of M_w). In order to determine A_2 by the latter procedure, we measured the reduced total intensity R_{Uv}^* of the unpolarized scattered light for vertically polarized incident light, ρ_u, the ratio $\kappa_T/\kappa_{T,0}$ of the isothermal compressibility κ_T of a given solution to that $\kappa_{T,0}$ of the solvent, and the refractive index increment $(\partial\tilde{n}/\partial c)_{T,p}$ at constant temperature T and pressure p for the oligomer solutions, and also the first two quantities for the solvent. The values of the refractive index $\tilde{n}$ at finite concentrations c, which were required to calculate K, were calculated with the values of the refractive index $\tilde{n}_0$ of the solvent and $(\partial\tilde{n}/\partial c)_{T,p}$ for each oligomer sample, as described in the next (Results) section. Measurements of R_{Uv}^* were carried out at scattering angles θ ranging from 45.0 to 142.5°, and the mean of values obtained at different θ was adopted as its value, since it must be independent of θ for oligomers. The values of ρ_u were obtained by the same method as that employed in the calibration of the apparatus.

Scattering data for the excess Rayleigh ratio ΔR_θ as a function of θ and c were analyzed by using the Berry-square-root plot[21] for the determination of $\langle S^2 \rangle$, and those for ΔR_0 at $\theta = 0$ as a function of c were analyzed by using the Bawn plot[22] for the determination of A_2. The correction for the anisotropic scattering was then applied to solutions of the samples with $M_w < 2 \times 10^3$.

The most concentrated solutions of the samples were prepared gravimetrically and made homogeneous by continuous stirring in the dark at ca. 50 °C for 3−7 days. The solutions were optically purified by filtration through a Teflon membrane of pore size 0.10, 0.45, or 1.0 μm. The solutions of lower concentrations were obtained by successive dilution. The weight fractions of the test solutions were converted to the polymer mass concentrations c by the use of the densities of the respective solutions calculated with the partial specific volumes v_2 of the samples and with the density ρ_0 of the solvent. The quantities v_2 and ρ_0 were measured with a pycnometer of the Lipkin−Davison type having a volume of 10 cm^3.

Isothermal Compressibility. Isothermal compressibility measurements were carried out to determine $\kappa_T/\kappa_{T,0}$ for the oligomer samples OAMS4 and OAMS5 in cyclohexane at 15.0 and 45.0 °C. The apparatus and the method of measurements are the same as those described in the previous paper.[11] The ratio $\kappa_T/\kappa_{T,0}$ was determined as a function of c and p. The latter was varied from 1 to ca. 50 atm. In this range of p, it was independent of p within experimental error, so that we adopted the mean of values obtained at various pressures as its value at 1 atm.

Refractive Index Increment. The refractive index increment $(\partial\tilde{n}/\partial c)_{T,p}$ was determined as a function of c and T for the samples OAMS4, OAMS5, OAMS8, OAMS13, OAMS33, OAMS67, AMS2, and AMS5 at temperatures ranging from 15.0 to 45.0 °C at wavelength of 436 nm by the use of a Shimadzu differential refractometer.

Results

Light Scattering from Solutions of Oligo(α-methylstyrene). We first give the values of $\kappa_T/\kappa_{T,0}$ and $(\partial\tilde{n}/\partial c)_{T,p}$ required to analyze the LS data for the two samples OAMS4 and OAMS5 with $M_w < 10^3$, as mentioned in the Experimental Section.

The values of $\kappa_T/\kappa_{T,0}$ obtained for the sample OAMS4 in cyclohexane are 0.908, 0.905, and 0.879 at $c = 0.1079$, 0.1407, and 0.1824 g/cm^3, respectively, at 15.0 °C, and 0.887, 0.870, and 0.858 at $c = 0.1046$, 0.1366, and 0.1773 g/cm^3, respectively, at 45.0 °C. Those for the sample OAMS5 in cyclohexane are 0.933 and 0.844 at $c =$ 0.1270 and 0.1708 g/cm^3, respectively, at 15.0 °C, and 0.895 and 0.855 at $c =$ 0.1232 and 0.1659 g/cm^3, respectively, at 45.0 °C. The results so obtained for these two samples may be represented by the equation linear in c as

$$\kappa_T/\kappa_{T,0} = 1 + kc \tag{1}$$

with $k = -0.75$ cm^3/g for $c \lesssim 0.18$ g/cm^3 independent of temperature in its range from 15.0 to 45.0 °C. We note that the previous results for $\kappa_T/\kappa_{T,0}$ for the sample OAMS5 in cyclohexane at 30.5 °C (Θ)[10] may be represented by the same equation.

From the values of $(\partial\tilde{n}/\partial c)_{T,p}$ at 436 nm obtained for the samples OAMS4 through AMS5 in cyclohexane at temperatures ranging from 15.0 to 45.0 °C, it has been found that $(\partial\tilde{n}/\partial c)_{T,p}$ for each sample may be represented by the equation linear in T as

$$(\partial\tilde{n}/\partial c)_{T,p} = k_1 + k_2(T - \Theta) \tag{2}$$

independent of c for $c \lesssim 0.18$ g/cm^3 and that the value of the coefficient k_2 is independent of M_w and is equal to $(4.3 \pm 0.5) \times 10^{-4}$ cm^3/g deg. The values of k_1, i.e., $(\partial\tilde{n}/\partial c)_{T,p}$ at the Θ temperature had already been determined for the samples OAMS5 through AMS5 in the previous studies[10,14] of $\langle S^2 \rangle$ and A_2, and are 0.169_4, 0.182_1, 0.188_0, 0.196_9, 0.201_2, 0.200_7, and 0.200_5 cm^3/g, respectively. The value of k_1 for the sample OAMS4 has been determined to be 0.157_6 cm^3/g in the present work. As for the samples with $M_w \gtrsim 10^5$, the values of k_1 and k_2 in cyclohexane at temperatures ranging from 25.0 to 55.0 °C are 0.203_7 cm^3/g and 4.3×10^{-4} cm^3/g deg,

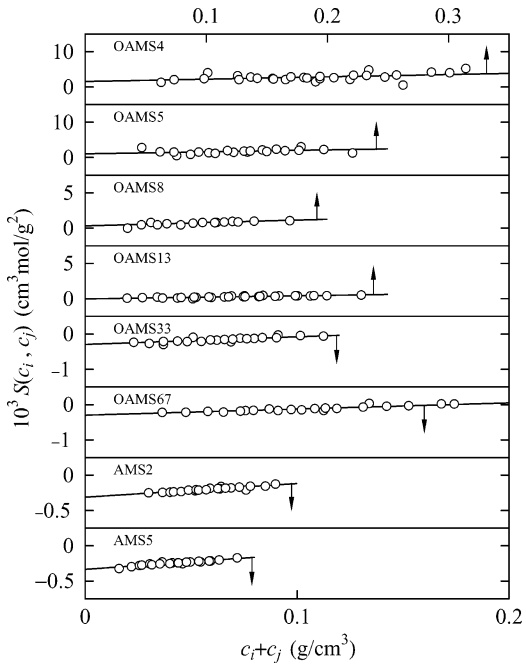

Figure 1. Bawn plots for the indicated a-PαMS samples in cyclohexane at 15.0 °C.

respectively, which have been evaluated from the empirical interpolation formula 2 of ref 10. We note that eq 2 with these values of k_1 and k_2 is also valid for solutions of the sample AMS15 at 20.0 °C. The value of $\tilde{n}$ for each sample at given c ($c \lesssim 0.18$ g/cm^3) and temperature may be calculated from

$$\tilde{n} = \tilde{n}_0 + (\partial\tilde{n}/\partial c)_{T,p}\, c \tag{3}$$

with the value of $(\partial\tilde{n}/\partial c)_{T,p}$ given by eq 2 and that of $\tilde{n}_0$ for pure cyclohexane calculated from an interpolation formula[23] as a function of temperature.

Now we may calculate the excess Rayleigh ratio ΔR_0 for all the samples, including the oligomers, by the use of the values of $\kappa_T/\kappa_{T,0}$ and $(\partial\tilde{n}/\partial c)_{T,p}$ obtained above. The Berry square-root plot[21] of $(Kc/\Delta R_0)^{1/2}$ against c for each a-PαMS sample in cyclohexane at each temperature has been found to follow a curve concave upward in the range of c studied, although not explicitly shown. This indicates that the third virial coefficient A_3' as well as the second virial coefficient A_2' contributes to$Kc/\Delta R_0$ as c is increased. (Here, the prime attached to A_2 and A_3 indicates that they are *light-scattering* virial coefficients.) It is then difficult to determine A_2' from the plots with high accuracy, so that we have made Bawn plots.[22]

Figure 1 shows Bawn plots for the indicated a-PαMS samples in cyclohexane at 15.0 °C, where $S(c_i, c_j)$ is defined by eq 4 of ref 10. As seen from the figure, the data points for each sample follow a straight line, indicating that the terms higher than A_3' may be neglected in the range of c studied. From the straight lines indicated, we have determined A_2' and A_3' for each sample in cyclohexane at 15.0 °C. Then we have determined M_w of each sample as before[1-3] so that the curve of $(Kc/\Delta R_0)^{1/2}$ calculated by the use of these values of M_w, A_2', and A_3' may give a best fit to the data points for each sample in the Berry square-root plot. The data at the other temperatures and also for the samples with higher molecular weights have been analyzed by the same method. Thus, the values of M_w, A_2', and A_3' for all the samples have been determined rather accurately. For the samples AMS40, AMS200, and AMS320 in cyclohexane at various temperatures ranging from 25.0 to 40.0 °C, we have also determined $\langle S^2\rangle$ from the Berry square-root plot.

The values of A_2' and A_3' so determined for each a-PαMS sample in cyclohexane may be equated to those of the (osmotic) second and third virial coefficients A_2 and A_3, respectively, as in the cases of the previous results at Θ and in good solvents.[10] We treat only the results for A_2 in the remainder of this paper, and we will analyze those for A_3 in a forthcoming paper.

Table 2. Results for A_2 of Atactic Oligo- and Poly(α-methylstyrene)s in Cyclohexane

	10^4A_2, cm^3 mol/g^2						
sample	15.0 °C	20.0 °C	25.0 °C	30.5 °C (Θ)	35.0 °C	40.0 °C	45.0 °C
OAMS4	7.75	11.0	13.0	16.5	18.8	21.0	23.0
OAMS5	5.25	7.75	10.0	12.5[a]	14.3	16.0	17.8
OAMS8	1.60	3.60	5.80	7.20	8.70	10.2	11.5
OAMS13	−0.15	1.40	2.70	4.00	4.90	5.70	6.80
OAMS33	−1.48	−0.50	0.37	1.00	1.63	2.18	2.65
OAMS67	−1.50	−0.82	−0.16	0.30	0.66	1.00	1.40
AMS2	−1.56	−1.12	−0.60	−0.15	0.20	0.57	0.89
AMS5	−1.67	−1.20	−0.70	−0.28	0.11	0.42	0.73
AMS15		−1.08	−0.57	−0.15	0.16	0.40	0.63

[a] A_2's for OAMS5 through AMS15 at 30.5 °C have been taken from ref 10.

Second Virial Coefficient and Gyration-Radius Expansion Factor. The values of A_2 so determined for the samples with $M_w < 2 \times 10^5$ in cyclohexane at temperatures ranging from 15.0 to 45.0 °C are given in Table 2. In Table 3 are given the values of A_2 along with those of α_S^2 for the samples with $M_w > 2 \times 10^5$ in cyclohexane at temperatures ranging from 25.0 to 45.0 °C. The values of A_2 for all the samples except OAMS4 at 30.5 °C (Θ) in Table 2 have been taken from Table 2 of ref 10, and those for all the three samples at 30.5, 35.0, and 45.0 °C in Table 3, from Table 3 of ref 10. The values of α_S^2 for all the three samples at 35.0 and 45.0 °C in Table 3 have been calculated from the defining equation

$$\langle S^2\rangle = \langle S^2\rangle_0 \alpha_S^2 \tag{4}$$

with the values of $\langle S^2\rangle$ given in Table 3 of ref 10 and the corresponding unperturbed values $\langle S^2\rangle_0$ given in Table 3 of ref 14. We note that LS data could not be obtained for test solutions of the sample AMS15 at 15.0 °C and of the samples AMS200 and AMS320 at 25.0 °C since phase separation occurred for them in the range of c in which LS measurements were carried out.

Figure 2 shows plots of A_2 against log M_w in cyclohexane at 45.0, 40.0, 35.0, 30.5 (Θ), 25.0, 20.0, and 15.0 °C from top to bottom. The data points at 45.0, 40.0, and 35.0 °C are shifted upward by 3×10^{-4}, 2×10^{-4}, and 1×10^{-4} cm^3 mol/g^2, respectively, and those at 25.0, 20.0, and 15.0 °C, downward by1×10^{-4}, 2×10^{-4}, and 3×10^{-4} cm^3 mol/g^2, respectively. The plot at 30.5 °C includes the values 5.60×10^{-4}, 2.35×10^{-4}, 1.75×10^{-4}, 5.5×10^{-5}, 8×10^{-6}, -2.6×10^{-5}, -1.2×10^{-5}, -6×10^{-6}, 0, and 0 cm^3 mol/g^2 of A_2 previously[10] determined for the a-PαMS samples with $M_w = 1.27 \times 10^3$, 2.27×10^3, 2.96×10^3, 4.57×10^3, 1.30×10^4, 6.46×10^4, 1.15×10^5, 2.38×10^5, 8.50×10^5, and 5.46×10^6, respectively, in addition to those given in Tables 2 and 3. The heavy solid curve connects smoothly the data

Table 3. Results for A_2 and α_S^2 of Atactic Poly(α-methylstyrene) in Cyclohexane

sample	25.0 °C	27.0 °C	28.0 °C	29.0 °C	30.5 °C (Θ)	33.0 °C	35.0 °C	40.0 °C	45.0 °C
					$10^4 A_2$, cm^3 mol/g^2				
AMS40	−0.43	−0.28	−0.20	−0.15	0[a]	0.13	0.20[a]	0.39	0.55[a]
AMS200		−0.30	−0.21	−0.10	0	0.11	0.18	0.30	0.41
AMS320		−0.35	−0.21	−0.13	0	0.10	0.17	0.28	0.37
					α_S^2				
AMS40	0.86_1	0.90_6	0.94_1	0.96_4	1	1.04_1	1.07_1[b]	1.13_1	1.16_7[b]
AMS200		0.81_9	0.88_1	0.91_4	1	1.10_1	1.15_5	1.27_4	1.35_1
AMS320		0.81_0	0.86_4	0.91_8	1	1.12_5	1.19_3	1.29_9	1.43_7

[a] A_2's for all the three samples at 30.5, 35.0, and 45.0 °C have been taken from ref 10. [b] α_S^2's for all the three samples at 35.0 and 45.0 °C have been calculated from the values of $\langle S^2 \rangle$ given in ref 10 and those of $\langle S^2 \rangle_0$ given in ref 14.

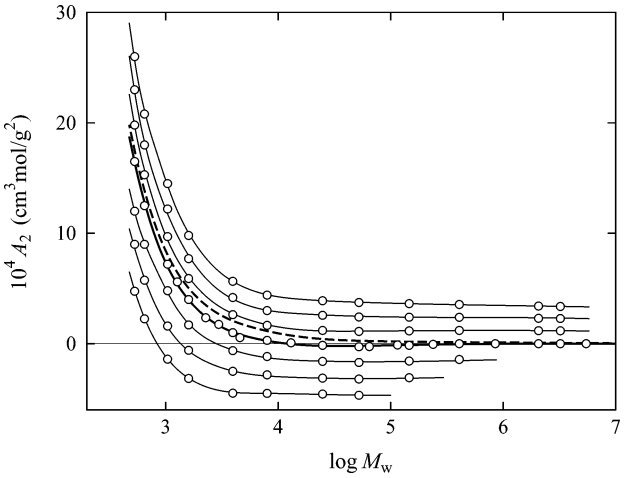

Figure 2. Plots of A_2 against log M_w for a-PαMS in cyclohexane at 45.0, 40.0, 35.0, 30.5 (Θ), 25.0, 20.0, and 15.0 °C from top to bottom. The data points at 45.0, 40.0, and 35.0 °C are shifted upward by 3×10^{-4}, 2×10^{-4}, and 1×10^{-4} cm^3 mol/g^2, respectively, and those at 25.0, 20.0, and 15.0 °C, downward by 1×10^{-4}, 2×10^{-4}, and 3×10^{-4} cm^3 mol/g^2, respectively. The heavy solid curve connects smoothly the data points at 30.5 °C, and the light solid curves connect smoothly those at the other temperatures. The heavy dashed curve represents the values of A'_2 ($=A_2 - A_{2,\beta_3}^{(HW)}$) associated with those of A_2 at 30.5 °C (see the text).

points at 30.5 °C (Θ), and the light solid curves connect smoothly those at the other temperatures. The heavy dashed curve represents the values of a quantity A'_2 ($= A_2 - A_{2,\beta_3}^{(HW)}$) (not to be confused with the light-scattering A_2), which are associated with those of A_2 at Θ and are estimated and discussed in the next (Discussion) section. The rapid decrease in A_2 with increasing M_w for small M_w at each temperature is due to the effects of chain ends.[4,24] As pointed out in the previous paper,[10] A_2 at 30.5 °C (Θ) then decreases slowly (from zero) to a negative minimum at $M_w \simeq 5 \times 10^4$. The plots at 25.0 and 20.0 °C have a similar feature. This may be regarded as arising from the effects of three-segment interactions.[7,8,10]

Discussion

Effects of Chain Ends on A_2. We analyze the data for A_2 shown in Figure 2 by the use of the HW theory[4,8,24] that takes account of both effects of chain stiffness and chain ends, and also of those of three-segment interactions at the Θ temperature, on the basis of the HW bead model. For convenience, we begin by summarizing necessary basic equations. The model is such that $n + 1$ beads are arrayed with spacing a between them along the contour of total length $L = na$, where $n - 1$ intermediate beads are identical and the two end beads are different from the intermediate ones and also from each other in species. Identical excluded-volume interactions between intermediate beads are expressed in terms of the *effective* binary-cluster integral β, which is redefined so as to include the contribution of three-segment interactions (ternary-cluster integral β_3).[4,8,9] In addition to β, two kinds of (effective) excess binary-cluster integrals $\beta_{2,1}$ and $\beta_{2,2}$ are introduced to express interactions between unlike beads, $\beta_{2,1}$ being associated with one end bead and $\beta_{2,2}$ with two end ones. The HW model itself is defined in terms of three basic model parameters: the constant differential-geometrical curvature κ_0 and torsion τ_0 of its characteristic helix and static stiffness parameter λ^{-1}.

According to the theory, A_2 may be written in the form

$$A_2 = A_2^{(HW)} + A_2^{(E)} \tag{5}$$

where $A_2^{(HW)}$ is the part of A_2 without the effects of chain ends, and $A_2^{(E)}$ represents their contribution to A_2 (from $\beta_{2,1}$ and $\beta_{2,2}$). The first term $A_2^{(HW)}$ may be written as

$$A_2^{(HW)} = A_{2,\beta}^{(HW)} + A_{2,\beta_3}^{(HW)} \tag{6}$$

where $A_{2,\beta}^{(HW)}$ is the part of $A_2^{(HW)}$ arising from β, which vanishes at Θ, and $A_{2,\beta_3}^{(HW)}$ is the residual contribution to $A_2^{(HW)}$ from β_3. Note that in the binary cluster approximation, the term $A_{2,\beta_3}^{(HW)}$ does not appear, so that $A_2^{(HW)} = A_{2,\beta}^{(HW)}$.[4,24] $A_{2,\beta}^{(HW)}$ (at $\beta \neq 0$) may be given by

$$A_{2,\beta}^{(HW)} = (N_A c_\infty^{3/2} L^2 B / 2M^2)\, h \tag{7}$$

where N_A is the Avogadro constant, and the constant c_∞ and the excluded-volume strength B are defined by

$$c_\infty = \frac{4 + (\lambda^{-1}\tau_0)^2}{4 + (\lambda^{-1}\kappa_0)^2 + (\lambda^{-1}\tau_0)^2} \tag{8}$$

and

$$B = \beta / a^2 c_\infty^{3/2} \tag{9}$$

Below or near Θ ($z < 0$ or very small $|z|$), the so-called h function on the right-hand side of eq 7 may be expanded as[25]

$$h = 1 - 2.865\tilde{z} + 8.851\tilde{z}^2 + 5.077\tilde{z}\tilde{\tilde{z}} - \ldots \tag{10}$$

where the intramolecular and intermolecular scaled excluded-volume parameters $\tilde{z}$ and $\tilde{\tilde{z}}$ are defined by

$$\tilde{z} = {}^3/_4 K(\lambda L)z \tag{11}$$

$$\tilde{\tilde{z}} = [Q(\lambda L)/2.865]z \tag{12}$$

with K and Q being functions only of λL and given by eq 8.46 of ref 4 (or eq 50 of ref 26) and by eq 8.102 of ref 4 (or eq 19 of ref 24) for $\lambda L \gtrsim 1$ (for ordinary flexible polymers), respectively. The conventional excluded-volume parameter z above is now defined by

$$z = (3/2\pi)^{3/2}(\lambda B)(\lambda L)^{1/2} \tag{13}$$

Above Θ ($z > 0$), h is given by eq 8.110 of ref 4 (or eq 18 of ref 24).

Thus, note that h is a function of $\tilde{z}$ and $\tilde{\tilde{z}}$ for $z > 0$ and $z < 0$ and that we may put $h = 1$ approximately for $\lambda L \lesssim 1$. Recall that L is related to M by the equation

$$L = M/M_L \tag{14}$$

with M_L being the shift factor, defined as the molecular weight per unit contour length.

The second term $A_{2,\beta_3}^{(HW)}$ on the right-hand side of eq 6 is a function of β_3, so that it in general depends on temperature if β_3 varies with temperature near Θ. On the experimental side, Nakamura et al.[27] have reported that β_3 is independent of temperature near Θ for PS in *trans*-decalin. We assume that this is also the case with a-PαMS in cyclohexane, although there is no experimental report on it, and equate $A_{2,\beta_3}^{(HW)}$ to the term $A_2^{(HW)}$ at Θ at which $A_{2,\beta}^{(HW)}$ vanishes. Denoting $A_2^{(HW)}$ at Θ by $A_{2,\Theta}^{(HW)}$, we then have

$$A_{2,\beta_3}^{(HW)} = A_{2,\Theta}^{(HW)} \tag{15}$$

The quantity $A_{2,\Theta}^{(HW)}$ may be given by[8]

$$A_{2,\Theta}^{(HW)} = -\frac{3A_3^0(\lambda/M_L)^{1/2}}{8\pi^{3/2}N_A(\langle S^2\rangle_0/M)_\infty^{3/2}}[I(\infty) - I(\lambda L)] \tag{16}$$

where A_3^0 is the third virial coefficient without the effects of chain ends at the Θ temperature,[4,28] $(\langle S^2\rangle_0/M)_\infty$ is the value of $\langle S^2\rangle_0/M$ in the limit of $M \to \infty$, and I is a function only of λL and is given by eq 36 of ref 8.

The second term $A_2^{(E)}$ on the right-hand side of eq 5 may be written in the form[4,24]

$$A_2^{(E)} = a_1 M^{-1} + a_2 M^{-2} \tag{17}$$

where

$$a_1 = 2N_A\beta_{2,1}/M_0$$
$$a_2 = 2N_A\Delta\beta_{2,2} \tag{18}$$

with M_0 the molecular weight of the bead and with

$$\Delta\beta_{2,2} = \beta_{2,2} - 2\beta_{2,1} \tag{19}$$

The excess binary-cluster integrals $\beta_{2,1}$ and $\beta_{2,2}$ are explicitly defined in eqs 8.117 of ref 4 (or eq 22 of ref 24, in which the symbols β_1 and β_2 are used in place of $\beta_{2,1}$ and $\beta_{2,2}$, respectively).

In order to determine the values of a_1 and a_2, it is convenient to introduce the quantity A'_2 defined by

$$A'_2 = A_2 - A_{2,\beta_3}^{(HW)} \tag{20}$$

In the oligomer region, where the relation $h = 1$ holds, $A_{2,\beta}^{(HW)}$ is independent of M, so that we have, from eqs 5, 6, 17, and 20

$$(A'_{2,i} - A'_{2,j})/(M_i^{-1} - M_j^{-1}) = a_1 + a_2(M_i^{-1} + M_j^{-1}) \tag{21}$$

where $A'_{2,i}$ and $A'_{2,j}$ denote the values of A'_2 for the samples with different molecular weights M_i and M_j, respectively. Equation 21 indicates that a_1 and a_2 may be determined from the intercept and slope of the plot of $(A'_{2,i} - A'_{2,j})/(M_{w,i}^{-1} - M_{w,j}^{-1})$ vs $(M_{w,i}^{-1} + M_{w,j}^{-1})$, respectively. Figure 3 shows such plots with the present data for the low-molecular-weight samples with $M_w \le 3.95 \times 10^3$, for which h may be equated to unity, at the indicated temperatures. Here, the values of A'_2 have been calculated from eq 20 with the observed values of A_2 and with the theoretical values of $A_{2,\beta_3}^{(HW)}$ calculated from eq 15 with eq 16 with the respective values 46.8 Å and 39.8 Å^{-1} of λ^{-1} and M_L previously[14] determined from $\langle S^2\rangle_0$ and with the respective observed values $6.8_2 \times 10^{-18}$ cm^2 mol/g and 5.0×10^{-4} cm^6 mol/g^3 of $(\langle S^2\rangle_0/M_w)_\infty$ and A_3^0 previously[10,14] obtained. We note that only the values of A'_2 so calculated at 30.5 °C (Θ) have been plotted in Figure 2 (dashed line), for simplicity. The data points in Figure 4 at each temperature can be fitted by a straight line. The results confirm that the upswing of A_2 for small M_w shown in Figure 2 arises from the effect of chain ends. From the straight lines indicated, we have determined a_1 and a_2 at the respective temperatures.

Figure 4 shows plots of A'_2 against M_w^{-1} with the data corresponding to those in Figure 3. From the plots, we have determined $A_{2,\beta}^{(HW)}$ with $h = 1$ at each temperature so that the curve of A'_2 ($= A_{2,\beta}^{(HW)} + A_2^{(E)}$) as a function of M_w^{-1} calculated from eqs 5, 6, 17, and 20 with these values of $A_{2,\beta}^{(HW)}$ (with $h = 1$), a_1, and a_2 gives a best fit to the data points. The curves in Figure 4 represent the values so calculated. The good agreement between the calculated and observed values indicates again that the dependence of A_2 on M_w for low M_w arises from the effect of chain ends. Note that the intercept of each curve is equal to $A_{2,\beta}^{(HW)}$ with $h = 1$, i.e., the prefactor $(N_A c_\infty^{3/2} L^2 B/2M^2)$, from which we have determined B at the corresponding temperature.

Temperature Dependence of Effective Binary-Cluster Integrals. With the values of B, a_1, and a_2 obtained in the last subsection, we have calculated β, $\beta_{2,1}$, and $\beta_{2,2}$ at the respective temperatures from eqs 9 and 18 with eq 19 (and with $a = M_0/M_L$) by taking the repeat unit of the chain as a single bead ($M_0 = 118$). For the calculation of β, we have used the above-mentioned values of λ^{-1} and M_L along with the respective values 3.0 and 0.9 of $\lambda^{-1}\kappa_0$ and $\lambda^{-1}\tau_0$.

The values of β (in Å^3) obtained at various temperatures above and below Θ are represented by the unfilled circles in Figure 5. It is clearly seen that the present data points for τ ($= 1 - \Theta/T$) < 0 deviate downward from a linear extension of the straight line fitted to the data points for $\tau > 0$ (dashed line). The values of β may

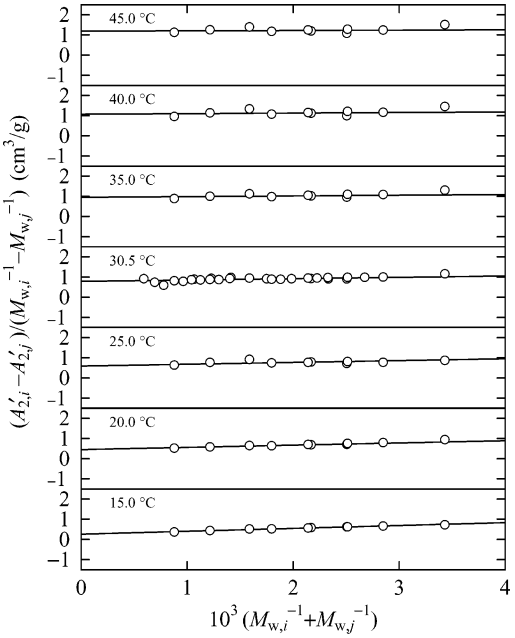

Figure 3. Plots of $(A'_{2,i} - A'_{2,j})/(M_{w,i}^{-1} - M_{w,j}^{-1})$ against $M_{w,i}^{-1} + M_{w,j}^{-1}$ for a-PαMS in cyclohexane at the indicated temperatures (see the text).

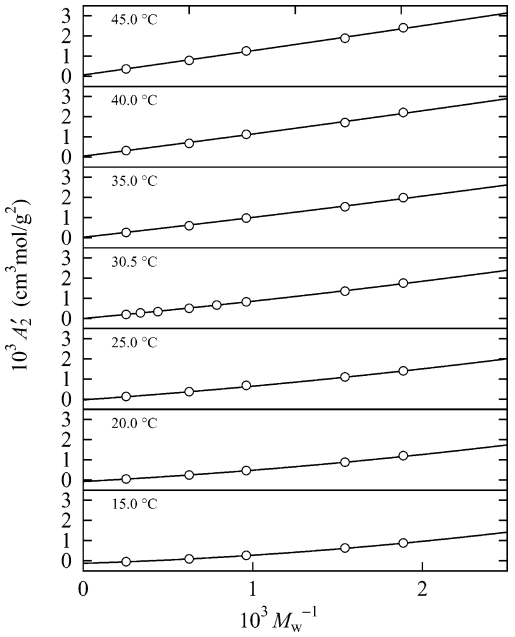

Figure 4. Plots of A'_2 against M_w^{-1} for a-PαMS in cyclohexane at the indicated temperatures (see the text).

be well reproduced by an empirical equation as a function of τ as follows

$$\beta = 66\tau \quad \text{for} \quad \tau \geq 0$$
$$= 66\tau - 830\tau^2 \quad \text{for} \quad \tau < 0 \tag{22}$$

The solid curve in Figure 5 represents the values calculated from these equations.

In Figure 6, the values of $\beta_{2,1}$ (unfilled circles) and $\beta_{2,2}$ (filled circles) are plotted against τ. They are of reasonable order of magnitude as the effective excess binary-cluster integrals associated with the chain end beads compared to those for small molecules.[29] The data points for $\beta_{2,1}$ follow a curve convex upward, while those for $\beta_{2,2}$ follow a curve concave upward. With these

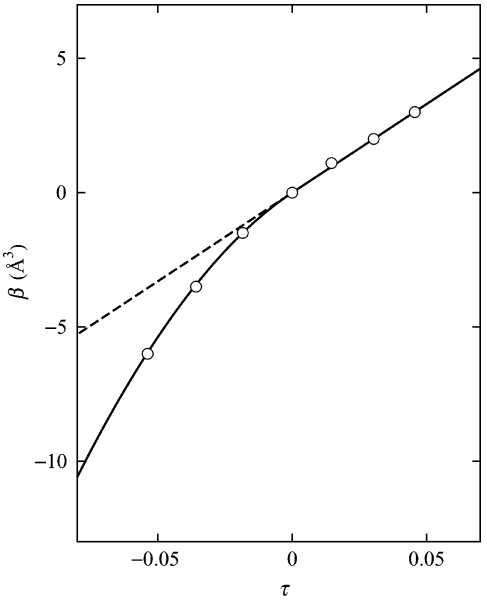

Figure 5. Plots of β against $\tau = 1 - \Theta/T$ for a-PαMS in cyclohexane with the β values from A_2. The solid curve represents the values calculated from eqs 22, and the dashed straight line is an extension of the solid straight line for $T > \Theta$ (see the text).

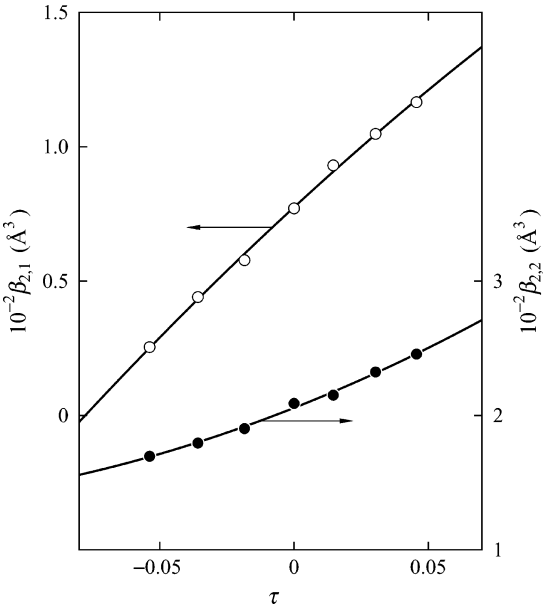

Figure 6. Plots of $\beta_{2,1}$ and $\beta_{2,2}$ against $\tau = 1 - \Theta/T$ for a-PαMS in cyclohexane: (○) $\beta_{2,1}$; (●) $\beta_{2,2}$. The solid curves for $\beta_{2,1}$ and $\beta_{2,2}$ represent the values calculated from eqs 23 and 24, respectively.

results, for later use, we have also constructed empirical equations for $\beta_{2,1}$ and $\beta_{2,2}$ (both in Å^3) as functions of τ as follows

$$\beta_{2,1} = 78 + 920\tau - 970\tau^2 \tag{23}$$

$$\beta_{2,2} = 206 + 790\tau + 2100\tau^2 \tag{24}$$

The curves for $\beta_{2,1}$ and $\beta_{2,2}$ in Figure 6 represent the values calculated from eqs 23 and 24, respectively.

Dependence of $A_2M_w^{1/2}$ and $A_{2,\beta}^{(HW)}M_w^{1/2}$ on z. Now we examine the behavior of the quantities $A_2M_w^{1/2}$ and $A_{2,\beta}^{(HW)}M_w^{1/2}$ as functions of z. Figure 7 shows plots of $A_2M_w^{1/2}$ against z with all the data given in Tables 2

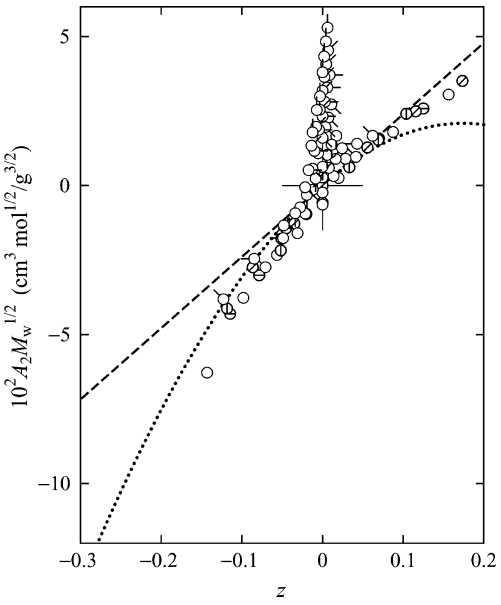

Figure 7. Plots of $A_2 M_w^{1/2}$ against z for a-PαMS in cyclohexane: unfilled circle with pip up, OAMS4; successive 45° clockwise rotations of pips correspond to OAMS5, OAMS8, OAMS13, OAMS33, OAMS67, AMS2, and AMS5, respectively; (Φ) AMS15; (∅) AMS40; (⊖) AMS200; (○) AMS320. The dashed and dotted curves represent the theoretical values with $A_2^{(E)} = A_{2,\beta_3}^{(HW)} = 0$ and $h = 1$ and the first-order TP perturbation theory values, respectively (see the text).

and 3, where values of z have been calculated from eq 13 with eqs 9 and 22 and with the above-mentioned values of the HW model parameters. The dashed straight line represents the theoretical values calculated from

$$A_{2,\beta}^{(HW)} M^{1/2} = A_2^0 z h \tag{25}$$

with $h = 1$ (the TP theory single-contact term), assuming that $A_2^{(E)} = A_{2,\beta_3}^{(HW)} = 0$, where A_2^0 is given by

$$A_2^0 = 4(\pi/6)^{3/2} N_A (c_\infty/\lambda M_L)^{3/2} \tag{26}$$

and is calculated to be 0.239 cm^3 mol$^{1/2}$/g$^{3/2}$ with the above-mentioned values of the HW model parameters. The dotted curve represents the values calculated from eq 25 with the first-order TP perturbation theory of h given by eq 10 with $\tilde{z} = \tilde{\tilde{z}} = z$ (i.e., $h = 1 - 2.865z$). The data points for the oligomer samples with very small M_w are seen to deviate extraordinarily upward from the dashed line around $z = 0$, and it turns out that all the data points cannot form a single-composite curve. This is due to the effects of chain ends.

With the above results for $\beta_{2,1}$ and $\beta_{2,2}$, we may estimate the contribution $A_2^{(E)}$ of the effects of chain ends to A_2 from eq 17 with eqs 18, 19, 23, and 24, and therefore $A_2^{(HW)}$ without these effects by subtracting the value of $A_2^{(E)}$ so obtained from the observed value of A_2. We may then estimate the part $A_{2,\beta}^{(HW)}$ of A_2 without the effects of three-segment interactions and also of chain ends by subtracting the above-calculated theoretical value of $A_{2,\beta_3}^{(HW)}$ from the value of $A_2^{(HW)}$ so obtained. Figure 8 shows plots of $A_{2,\beta}^{(HW)} M_w^{1/2}/A_2^0$ against the same z as in Figure 7. Here, the symbols and the lines have the same meaning as those in Figure 7. For comparison, the results (filled circles) obtained from a reanalysis of

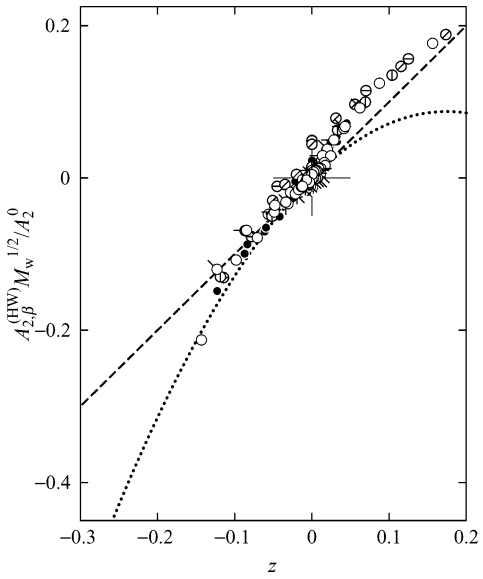

Figure 8. Plots of $A_{2,\beta}^{(HW)} M_w^{1/2}/A_2^0$ against z: (Φ, ∅, ⊖, ○ with and without pip) present data for a-PαMS in cyclohexane (the symbols and the lines have the same meaning as those in Figure 7); (●) previous data for a-PS with M_w from 3.70×10^2 to 4.00×10^4 in cyclohexane.[1]

the previous data for a-PS samples with $3.70 \times 10^2 \le M_w \le 4.00 \times 10^4$ in cyclohexane near the Θ temperature[1] in the same manner as above are also shown in Figure 8. We omit the details of the reanalysis and only give the values of the HW model parameters and related quantities required for it:[4,28,30] $\lambda^{-1} = 20.6$ Å, $M_L = 35.8$ Å^{-1}, $\lambda^{-1}\kappa_0 = 3.0$, $\lambda^{-1}\tau_0 = 6.0$,$(\langle S^2\rangle_0/M_w)_\infty = 7.8_2 \times 10^{-18}$ cm^2 mol/g, and $A_3^0 = 4.7 \times 10^{-4}$ cm^6 mol/g^3. The value of A_2^0 necessary for the plot for a-PS has been calculated to be 0.294 cm^3 mol$^{1/2}$/g$^{3/2}$.

It is seen that the extraordinary deviation of the $A_2 M_w^{1/2}$ vs z plot upward from the dashed line around $z = 0$ found in Figure 7 disappears in Figure 8 and that all the data points along with those for a-PS nearly form a single-composite curve. Thus, the previous conclusion derived without consideration of the effects of three-segment interactions is still valid; that is, the effect of chain stiffness on $A_{2,\beta}^{(HW)}$ and hence A_2 is of little significance below Θ in contrast to the behavior of A_2 above Θ, or in other words, the TP theory prediction is valid for $A_{2,\beta}^{(HW)}$ below Θ irrespective of the difference in polymer species.

It should be noted here that the data points in Figure 8 for the samples with $M_w \gtrsim 10^5$ deviate somewhat upward from the dashed line in the range of $z > 0$. As pointed out in the previous papers,[8,10] the convergence of the theoretical $A_{2,\beta_3}^{(HW)}$ to zero with increasing M is rather slow ($\propto M^{-1/2}$), and there still remains a small but finite negative value even for such large M_w where the observed A_2 at Θ vanishes. This indicates that the theory is not complete as yet. Thus, the values of A'_2 with the correction of $A_{2,\beta_3}^{(HW)}$, as shown in Figure 2 (dashed line) for the case at 30.5 °C, and therefore those of $A_{2,\beta}^{(HW)}$ may be somewhat overestimated, especially in the range of large M_w.

Dependence of α_S on $\tilde{z}$. Figure 9 shows plots of α_S^2 against $\tilde{z}$, where values of $\tilde{z}$ have been calculated from eq 11 with eq 8.46 of ref 4 for K and with the values of z calculated as above. The circles with slash bar, the circles with horizontal bar, and the unfilled circles

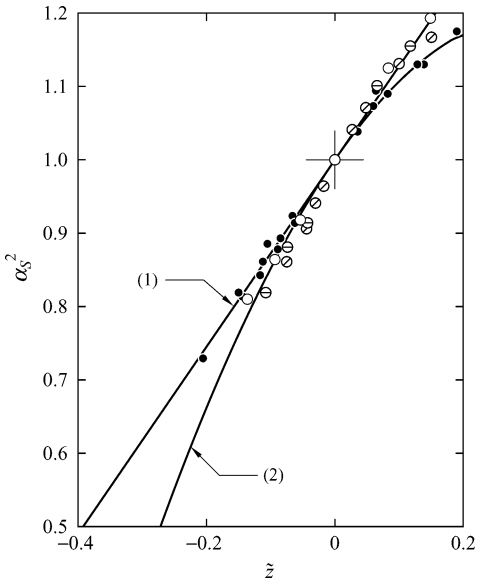

Figure 9. Plots of α_S^2 against $\tilde{z}$: (∅, ⊖, ○) present data for a-PαMS in cyclohexane (the symbols have the same meaning as those in Figure 7); (●) previous data for a-PS with M_w from 1.27×10^6 to 6.40×10^6 in cyclohexane.[31] Curves 1 and 2 represent the first- and second-order perturbation theory values, respectively.

represent the present values for the samples AMS40, AMS200, and AMS320, respectively, in cyclohexane. For comparison, the results (filled circles) previously[31] obtained for a-PS samples with $1.27 \times 10^6 \leq M_w \leq 6.40 \times 10^6$ in cyclohexane are also shown in Figure 9. We note that we have used the values of $\tilde{z}$ recalculated for a-PS with the values of β determined from the above-mentioned reanalysis. The curves (1) and (2) represent the first- and second-order perturbation theory values, respectively, calculated from

$$\alpha_S^2 = 1 + 1.276\,\tilde{z} - 2.082\,\tilde{z}^2 + \ldots \qquad (27)$$

It is seen that all the data points nearly form a single-composite curve within experimental error. This confirms that the QTP theory is valid for α_S below Θ as well as above Θ irrespective of the difference in polymer species as in the previous analysis without consideration of three-segment interactions.

Finally, we make some comments on the effects of three-segment interactions on A_2 and α_S from a theoretical point of view. As mentioned in the previous paper,[8] three-segment interactions (β_3) have also an effect on $\langle S^2\rangle_0$ at Θ ($\beta = 0$), making the theoretical value of $\langle S^2\rangle_0$ somewhat smaller than the conventional one evaluated in the binary cluster approximation ($\beta_3 = 0$). As a result, it seems necessary to make a correction to the relation between α_S and β, as done to that between A_2 and β in the present work. Then the value of β determined from A_2 with the correction does not necessarily agree with that from α_S without it. Fortunately, however, such a difference in β proves to be negligibly small for the polymer−solvent systems studied, since the variations themselves of A_2 and α_S with β and hence also the correlation between them hardly alter even with the present correction to A_2 (below Θ), as seen from a comparison of Figures 8 and 9 with Figures 10 and 11 of ref 3.

Conclusion

For solutions of several a-PαMS samples, including the oligomers with very small M_w, in cyclohexane near the Θ temperature, the contribution $A_2^{(E)}$ of the effects of chain ends to the second virial coefficient A_2 has been successfully determined from the part A'_2 of A_2 without the effects of three-segment interactions. The part A'_2 has been estimated by subtracting the contribution $A_{2,\beta_3}^{(HW)}$ of these effects from the observed A_2, where $A_{2,\beta_3}^{(HW)}$ has been calculated by the use of the HW theory recently developed and on the assumption that the ternary cluster integral β_3 is independent of temperature near Θ. From the values of $A_2^{(E)}$ so determined at various temperatures, the effective excess binary-cluster integrals $\beta_{2,1}$ and $\beta_{2,2}$ associated with the chain end beads have been determined as functions of the absolute temperature T. Then, with these values of $\beta_{2,1}$ and $\beta_{2,2}$, the effective binary-cluster integral β between intermediate identical beads has been estimated as a function of T and found not to be proportional to $\tau = 1 - \Theta/T$ below Θ. With the values of β, the conventional and scaled excluded-volume parameters z and $\tilde{z}$ have been directly calculated without any assumption. The behavior of the part $A_{2,\beta}^{(HW)}$ ($= A_2 - A_2^{(E)} - A_{2,\beta_3}^{(HW)}$) of A_2 without the effects of chain ends and three-segment interactions as a function of z and also of the gyration-radius expansion factor α_S as a function of $\tilde{z}$ has been examined for the present results for a-PαMS along with the previous ones for a-PS, both in cyclohexane. It has then been found that the previous conclusions obtained without consideration of the effects of three-segment interactions, such as mentioned in the Introduction, are still valid.

Acknowledgment. This research was supported in part by the 21st century COE program COE for a United Approach to New Materials Science from the Ministry of Education, Culture, Sports, Science, and Technology, Japan.

References and Notes

(1) Yamakawa, H.; Abe, F.; Einaga, Y. *Macromolecules* **1994**, *27*, 5704.
(2) Abe, F.; Einaga, Y.; Yamakawa, H. *Macromolecules* **1995**, *28*, 694.
(3) Yamada, M.; Yoshizaki, T.; Yamakawa, H. *Macromolecules* **1998**, *31*, 7728.
(4) Yamakawa, H. *Helical Wormlike Chains in Polymer Solutions*; Springer: Berlin, 1997.
(5) Yamakawa, H. *Modern Theory of Polymer Solutions*; Harper & Row: New York, 1971. Its electronic edition is available on-line at the following URL: http://www.molsci.polym.kyoto-u.ac.jp/archives/redbook.pdf.
(6) Cherayil, B. J.; Douglas, J. F.; Freed, K. F. *J. Chem. Phys.* **1985**, *83*, 5293.
(7) Nakamura, Y.; Norisuye, T.; Teramoto, A. *Macromolecules* **1991**, *24*, 4904.
(8) Yamakawa, H.; Yoshizaki, T. *J. Chem. Phys.* **2003**, *119*, 1257.
(9) Yamakawa, H. *J. Chem. Phys.* **1966**, *45*, 2606.
(10) Tokuhara, W.; Osa, M.; Yoshizaki, T.; Yamakawa, H. *Macromolecules* **2003**, *36*, 5311.
(11) Einaga, Y.; Abe, F.; Yamakawa, H. *Macromolecules* **1993**, *26*, 6243.
(12) Abe, F.; Einaga, Y.; Yamakawa, H. *Macromolecules* **1994**, *27*, 3262.
(13) Li, J.; Harville, S.; Mays, J. W. *Macromolecules* **1997**, *30*, 466.
(14) Osa, M.; Yoshizaki, T.; Yamakawa, H. *Macromolecules* **2000**, *33*, 4828.
(15) Lindner, J. S.; Hadjichristidis, N.; Mays, J. W. *Polym. Commun.* **1989**, *30*, 174.

(16) Kojo, H.; Osa, M.; Yoshizaki, T.; Yamakawa, H. *Macromolecules* **2003**, *36*, 6570.
(17) Osa, M.; Sumida, M.; Yoshizaki, T.; Yamakawa, H.; Ute, K.; Kitayama, T.; Hatada, K. *Polym. J.* **2000**, *32*, 361.
(18) Deželić, Gj.; Vavra, J. *Croat. Chem. Acta* **1966**, *38*, 35.
(19) Rubingh, D. N.; Yu, H. *Macromolecules* **1976**, *9*, 681.
(20) Einaga, Y.; Abe, F.; Yamakawa, H. *J. Phys. Chem.* **1992**, *96*, 3948.
(21) Berry, G. C. *J. Chem. Phys.* **1966**, *44*, 4550.
(22) Bawn, C. E. H.; Freeman, R. F. J.; Kamalidin, A. R. *Trans. Faraday Soc.* **1950**, *46*, 862.
(23) Johnson, B. L.; Smith, J. In *Light Scattering from Polymer Solutions*; Huglin, M. B., Ed.; Academic Press: London, 1972; Chapter 2.
(24) Yamakawa, H. *Macromolecules* **1992**, *25*, 1912.
(25) Yamakawa, H. *Macromolecules* **1993**, *26*, 5061.
(26) Shimada, J.; Yamakawa, H. *J. Chem. Phys.* **1986**, *85*, 591.
(27) Nakamura, Y.; Inoue, N.; Norisuye, T.; Teramoto, A. *Macromolecules* **1997**, *30*, 631.
(28) Yamakawa, H.; Abe, F.; Einaga, Y. *Macromolecules* **1994**, *27*, 3272.
(29) Yamakawa, H.; Fujii, M. *J. Chem. Phys.* **1973**, *58*, 1523.
(30) Abe, F.; Einaga, Y.; Yoshizaki, T.; Yamakawa, H. *Macromolecules* **1993**, *26*, 1884.
(31) Arai, T.; Abe, F.; Yoshizaki, T.; Einaga, Y.; Yamakawa, H. *Macromolecules* **1995**, *28*, 5458.

MA035781D